Available online at www.sciencedirect.com
ScienceDirect
Bioorganic & Medicinal Chemistry 15 (2007) 295–304
Bioorganic & Medicinal Chemistry

Synthesis of β-ketophosphonate analogs of glutamyl and glutaminyl adenylate, and selective inhibition of the corresponding bacterial aminoacyl-tRNA synthetases

Christian Balg,[a,†] Sébastien P. Blais,[b,†] Stéphane Bernier,[a] Jonathan L. Huot,[b] Manon Couture,[b] Jacques Lapointe[b,*] and Robert Chênevert[a,*]

[a]*Département de chimie, Centre de recherche sur la fonction, la structure et l'ingénierie des protéines (CREFSIP), Faculté des sciences et de génie, Université Laval, Québec, Canada G1K 7P4*
[b]*Département de biochimie et de microbiologie, Centre de recherche sur la fonction, la structure et l'ingénierie des protéines (CREFSIP), Faculté des sciences et de génie, Université Laval, Québec, Canada G1K 7P4*

Received 4 August 2006; revised 21 September 2006; accepted 26 September 2006
Available online 29 September 2006

Abstract—The aminoacyl-β-ketophosphonate-adenosines (aa-KPA) are stable analogs of the aminoacyl adenylates, which are high-energy intermediates in the formation of aminoacyl-tRNA catalyzed by aminoacyl-tRNA synthetases (aaRS). We have synthesized glutamyl-β-ketophosphonate-adenosine (Glu-KPA) and glutaminyl-β-ketophosphonate-adenosine (Gln-KPA), and have tested them as inhibitors of their cognate aaRS, and of a non-cognate aaRS. Glu-KPA is a competitive inhibitor of *Escherichia coli* glutamyl-tRNA synthetase (GluRS) with a K_i of 18 μM with respect to its substrate glutamate, and binds at one site on this monomeric enzyme; the non-cognate Gln-KPA also binds this GluRS at one site, but is a much weaker (K_i = 2.9 mM) competitive inhibitor. By contrast, Gln-KPA inhibits *E. coli* glutaminyl-tRNA synthetase (GlnRS) by binding competitively but weakly at two distinct sites on this enzyme (average K_i of 0.65 mM); the non-cognate Glu-KPA shows one-site weak (K_i = 2.8 mM) competitive inhibition of GlnRS. These kinetic results indicate that the glutamine and the AMP modules of Gln-KPA, connected by the β-ketophosphonate linker, cannot bind GlnRS simultaneously, and that one Gln-KPA molecule binds the AMP-binding site of GlnRS through its AMP module, whereas another Gln-KPA molecule binds the glutamine-binding site through its glutamine module. This model suggests that similar structural constraints could affect the binding of Glu-KPA to the active site of mammalian cytoplasmic GluRSs, which are evolutionarily much closer to bacterial GlnRS than to bacterial GluRS. This possibility was confirmed by the fact that Glu-KPA inhibits bovine liver GluRS 145-fold less efficiently than *E. coli* GluRS by competitive weak binding at two distinct sites (average K_i = 2.6 mM). Moreover, these kinetic differences reveal that the active sites of bacterial GluRSs and mammalian cytoplasmic GluRSs have substantial structural differences that could be further exploited for the design of better inhibitors specific for bacterial GluRSs, promising targets for antimicrobial therapy.
© 2006 Elsevier Ltd. All rights reserved.

1. Introduction

Aminoacyl-tRNA synthetases (aaRSs) play a key role in protein biosynthesis in all living organisms. These enzymes catalyze the esterification of amino acids to cognate tRNA in a two-step process[1–3] (Scheme 1).

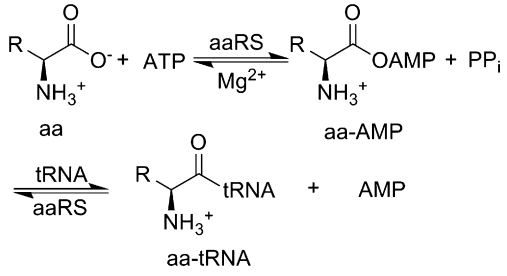

Scheme 1.

First, ATP reacts with the amino acid (aa) to form an enzyme-bound aminoacyl adenylate intermediate (aa-AMP) with displacement of pyrophosphate (PP_i).

Keywords: Aminoacyl-tRNA synthetases; Inhibitors; Aminoacyl adenylates; Analogs; β-Ketophosphonates.
* Corresponding authors. Tel.: +1 418 656 3283; fax: +1 418 656 7916 (R.C.); tel.: +1 418 656 2965; fax: +1 418 656 7176 (J.L.); e-mail addresses: jacques.lapointe@bcm.ulaval.ca; robert.chenevert@chm.ulaval.ca
† The two authors contributed equally to this work. C. B. for the organic synthesis part, and S. P. B. for the enzyme kinetics part.

0968-0896/$ - see front matter © 2006 Elsevier Ltd. All rights reserved.
doi:10.1016/j.bmc.2006.09.056

In aminoacyl adenylates, the high-energy mixed anhydride bond activates the carboxyl group of the amino acid. In the second step, the aminoacyl group is transferred to the 2′- or 3′-OH at the 3′ end of the tRNA, generating aminoacyl-tRNA (aa-tRNA) and adenosine monophosphate (AMP).

AaRSs are classified into two main groups of 10 enzymes each on the basis of common structural and mechanistic features.[3] GluRS and GlnRS belong to class I, whereas AspRS is a member of class II. GluRS and GlnRS have the characteristic, shared only by ArgRS and class I LysRS, of requiring the presence of their cognate tRNA to catalyze the activation of the amino acid substrate.[1]

Several natural products with various chemical structures have been identified as inhibitors of aaRSs.[4,5] These enzymes have been subjected to significant evolutionary divergence, and selective inhibition of bacterial enzymes has been observed. Pseudomonic acid, a secondary metabolite from *Pseudomonas fluorescens*, is the sole aaRS inhibitor currently used as an antibiotic.[6] This natural product is a potent (K_i = 6 nM for *E. coli* IleRS) and selective (10^4-fold selectivity for bacterial versus mammalian IleRS) inhibitor of bacterial IleRS.[7]

AaRSs are amenable to high throughput screening of compound libraries.[8] Rationally designed synthetic inhibitors of aaRS are typically stable analogs of aminoacyl adenylates (aa-AMP on Scheme 1).[4,5] The stability is achieved by replacement of the labile mixed anhydride function by non-hydrolyzable bioisosteres. Several aminoacylsulfamoyladenosines or aminoalkyl adenylates have been synthesized and shown to be inhibitors of corresponding aaRSs. The β-ketophosphonate function can also serve as a stable surrogate for the reactive acylphosphate subunit of aminoacyl adenylates in the design of aaRS inhibitors (Scheme 2).[9,10]

Herein we report the synthesis of β-ketophosphonate analogs of glutamyl and glutaminyl adenylates, and their interaction with their cognate aaRSs. We discuss the structural significance of the unusual kinetics of *E. coli* GlnRS inhibition by Gln-β-ketophosphonate and of a mammalian GluRS by Glu-β-ketophosphonate; we also underline the high specificity of Glu-β-ketophosphonate for a bacterial GluRS versus a mammalian cytoplasmic GluRS, and we discuss its interest for the design of novel antibiotics targeting bacterial GluRSs.

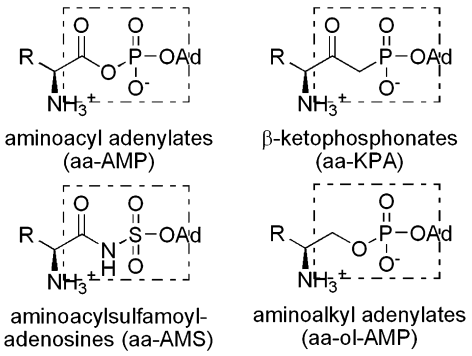

Scheme 2.

2. Results and discussion

2.1. Synthesis of β-ketophosphonates 4, 9, and 15

We recently reported the synthesis of ketophosphonate **4**.[9] This synthesis relied upon the activation of phosphonic monoester **2** with *p*-tosyl chloride in the presence of pyridine as a base, followed by condensation with isopropylideneadenosine **1** to give ketophosphonate **3** (Scheme 3). Although this condensation–deprotection reaction provided pure **3**, reaction times were long (14 days) and yields were low (30%). We sought to improve the synthesis of β-ketophosphonates, so we explored alternative strategies for the activation of phosphonic esters. The synthesis of glutamic ketophosphonate **9** is outlined in Scheme 4. Condensation of known glutamic ester **5**[11] with the lithium salt of dimethyl methylphosphonate provided β-ketophosphonate **6**. Phosphonic monoester **7** was obtained by selective demethylation of **6** with *tert*-butylamine.[12] The phosphonic ester **8** was obtained by esterification of **7** with isopropylideneadenosine **1** in the presence of *O*-benzotriazol-1-yl-*N*,*N*,*N*′,*N*′-tetramethyluronium hexafluorophosphate (HBTU) as a coupling reagent, followed by demethylation of the phosphonic methyl ester with pyridine/water at 55 °C.[13] Reaction of **8** with wet trifluoroacetic acid provoked the removal of the three remaining protecting groups (*tert*-butyl ester, *N*-Boc, and isopropylidene acetal) to give glutamic β-ketophosphonate **9**.

The synthesis of glutamine ketophosphonate **15** is summarized in Scheme 5. Glutamine methyl ester **11** was prepared by the reaction of the cesium salt of glutamine derivative **10** with CH_3I in DMF.[14] Condensation of ester **11** with the lithium anion of dimethyl methylphosphonate afforded dimethyl β-ketophosphonate **12**.[15] Selective monodemethylation of **12** with $PhSH/Et_3N$ provided monoester **13**. Esterification of phosphonic salt **13** with adenosine derivative **1** by the HBTU procedure, followed by demethylation of the phosphonic methyl ester, gave phosphonic ester **14**. We have observed that the intermediate phosphonic methyl ester is unstable but the corresponding salt **14** was easily isolated. The overall yield for this key two-step sequence was 57%. Treatment of **14** with CF_3COOH/H_2O resulted in simultaneous cleavage of the Boc, trityl, and isopropylidene groups to provide glutamine β-ketophosphonate **15**. This compound is stable in the solid state but decomposes slowly in solution.

2.2. Inhibition of *E. coli* GluRS by Glu-β-ketophosphonate-adenosine 9 (Glu-KPA) and specificity of this inhibition

The comparison of the double-reciprocal plots of the aminoacylation kinetic data at various concentrations of Glu-KPA (Fig. 1A) shows that it is essentially a competitive inhibitor of *E. coli* GluRS with respect to glutamate, as revealed by the intersection of the lines

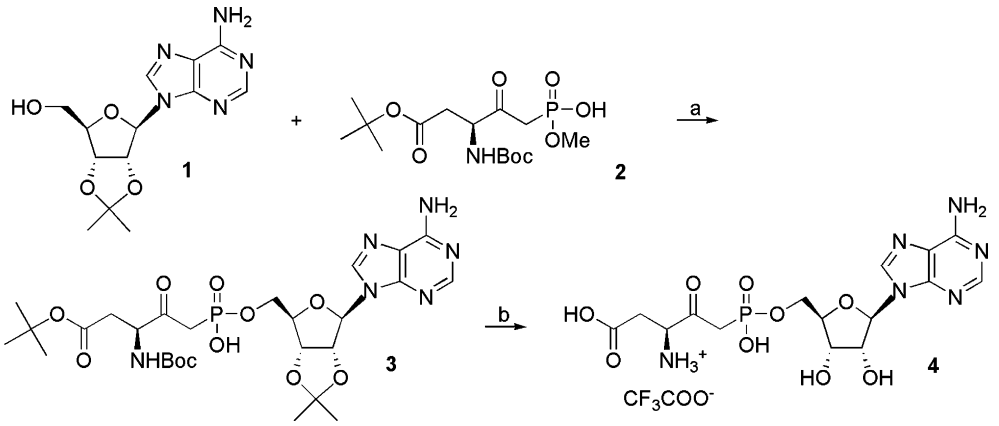

Scheme 3. Reagents and conditions: (a) TsCl, pyridine, rt, 14 days (b) CF_3COOH/H_2O, rt, 15 min.

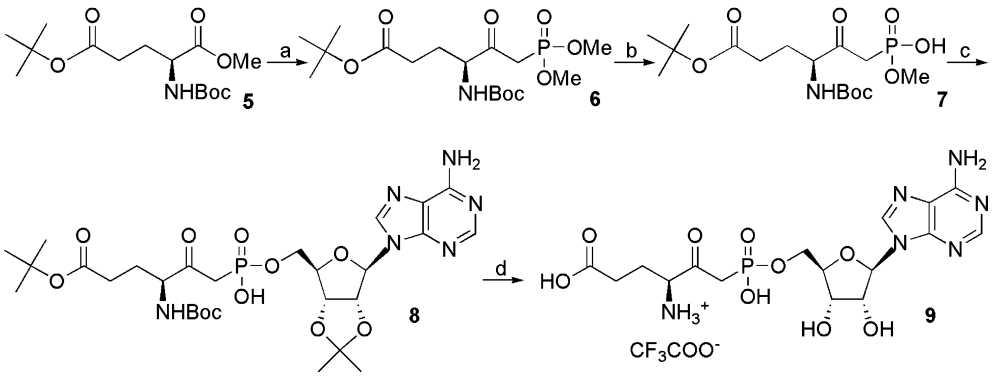

Scheme 4. Reagents and conditions: (a) $LiCH_2P(O)(OCH_3)_2$, THF, −78 °C, 1 h; (b) i—*t*-$BuNH_2$, reflux, 24 h; ii—HCl; (c) i—HBTU, *i*-Pr_2NEt, 2′,3′-isopropylideneadenosine **1**, DMF, rt, 8.5 h; ii—pyridine/H_2O, 55 °C, 10 h; (d) CF_3COOH/H_2O, rt, 15 min.

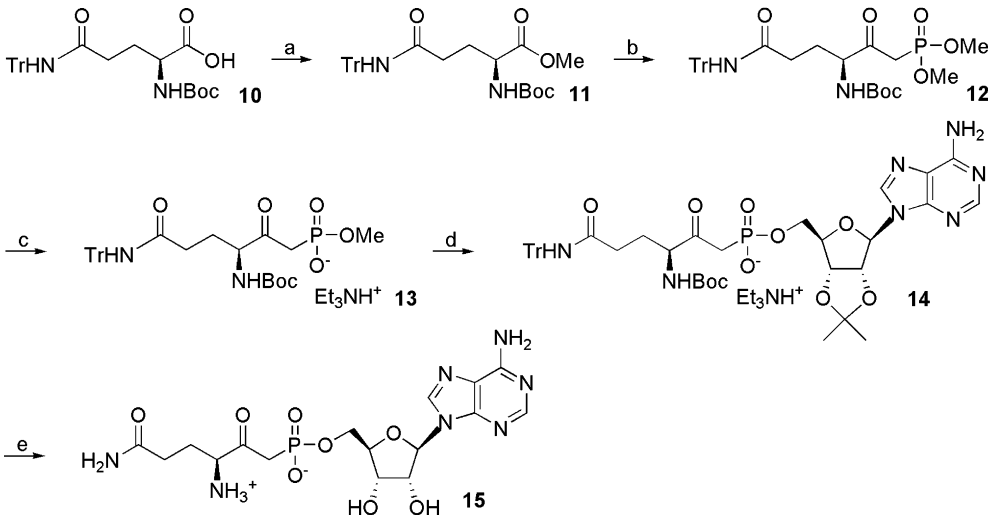

Scheme 5. Reagents and conditions: (a) i—Cs_2CO_3, MeOH/H_2O; ii—MeI, DMF, rt, 1 h; (b) $LiCH_2P(O)(OCH_3)_2$, THF, −78 °C, 2 h; (c) PhSH, Et_3N, THF/DMF, rt, 48 h; (d) i—HBTU, DMAP, 2′,3′-isopropylideneadenosine **1**, DMF, 3.5 h; ii—PhSH, Et_3N, DMF, rt, 24 h; (e) CF_3COOH/H_2O, rt, 15 min.

near the axis 1/[S] = 0. A K_i value of 18 μM was obtained from a replot of the slopes of the above-mentioned lines versus [inhibitor][16] (Fig. 1B). This competitive character of Glu-KPA inhibition with respect to glutamate is also revealed by the fitting of the kinetic relation $v_i/v_0 = f$ ([inhibitor]) with the competitive inhibition equation 1 (Fig. 2A, left curve; see Section 4). This curve-fitting procedure led to the same K_i value of 18 μM Glu-KPA (Fig. 1) for *E. coli* GluRS, and thus was used for identifying the other cases of competitive

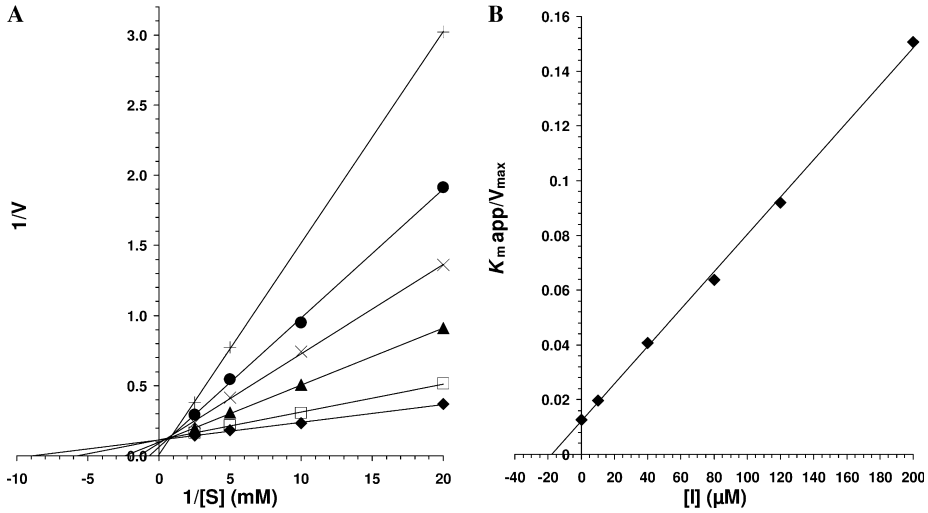

Figure 1. Inhibition of *Escherichia coli* GluRS by Glu-KPA **9**: (A) determination of the apparent K_m for glutamate in the presence of several concentrations of this inhibitor: 0 μM (♦), 10 μM (□), 40 μM (▲), 80 μM (×), 120 μM (●), and 200 μM (+). (B) Determination of the K_i value for this inhibitor with respect to glutamate, from the linear relation between the slopes of the reciprocal plots presented in A, as a function of the inhibitor concentration.

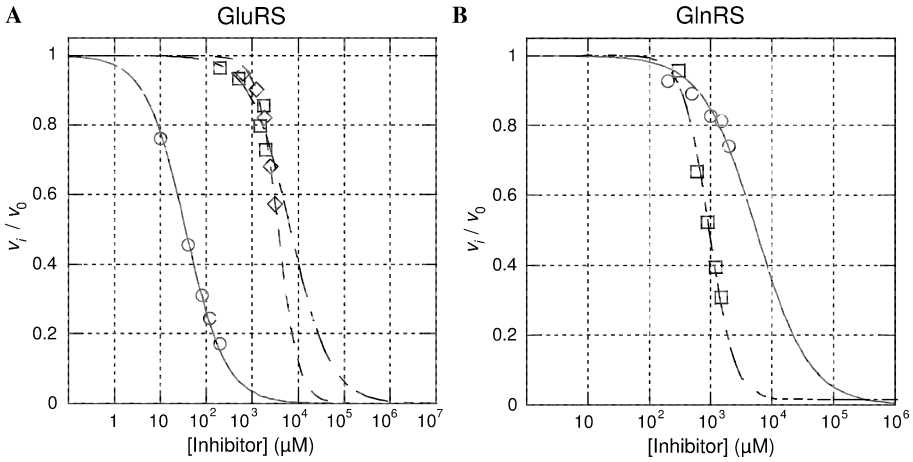

Figure 2. Inhibition by Glu-KPA **9** (○) and by Gln-KPA **15** (□) of: (A) *E. coli* GluRS; and inhibition of a mammalian GluRS by Glu-KPA **9** (◊); (B) *E. coli* GlnRS.

inhibition reported here, and for measuring the K_i values (Fig. 2, except for the left curve of Figure 2B). The related compound Gln-KPA **15**, which inhibits *E. coli* GlnRS (see below), evolutionarily related to GluRS[17], is a 170-fold weaker inhibitor (K_i = 2.9 mM) of *E. coli* GluRS (Fig. 2A, right curve, and Table 1) than is Glu-KPA.

2.3. Inhibition of *E. coli* GlnRS by Gln-β-ketophosphonate-adenosine 15 (Gln-KPA) and specificity of this inhibition

The kinetics of *E. coli* GlnRS inhibition by Gln-KPA (Fig. 2B) cannot be explained by a simple competitive inhibition, represented by the less tilted curve of $v_i/v_0 = f$([inhibitor]), but trace a steeper curve fitting correctly the data. As these aa-AMP analogs are made of two modules (aminoacyl and AMP), we considered the possibility that Gln-KPA binds at two sites on GlnRS, possibly the glutamine and the AMP sites, through its corresponding modules (Fig. 3). We thus used the mechanism of cooperative pure competitive inhibition by two different non-exclusive inhibitors[16] shown in Figure 4A, adapted to our situation where the two inhibitory components are part of the same Gln-KPA molecule. The velocity equation for this system under rapid equilibrium conditions, and the corresponding relation for

Table 1. K_i for the inhibition of various GluRS and of *E. coli* GlnRS by aa-AMP analogs

aa-AMP analog	*E. coli* GlnRS	*E. coli* GluRS	Mammalian liver GluRS	Ratio K_i mammalian/K_i *E. coli*	Ref.
Gln-KPA	0.65 mM	2.9 mM	ND	ND	This work
Glu-KPA	2.8 mM	18 μM	2.6 mM	145	This work
Glu-AMS	ND	2.8 nM	70 nM	25	25

ND, not determined.

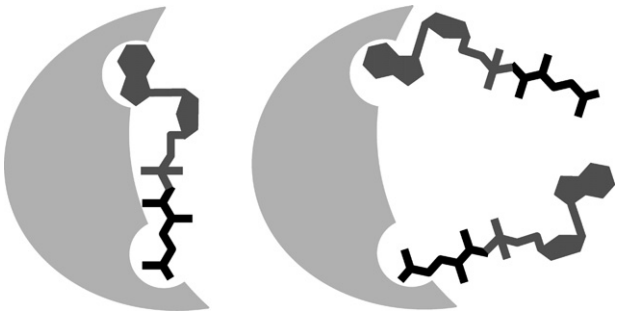

Figure 3. Schematic models of the binding of one molecule of aa-AMP to an aaRS (left) and of two molecules of Gln-KPA **15** to *E. coli* GlnRS (right).

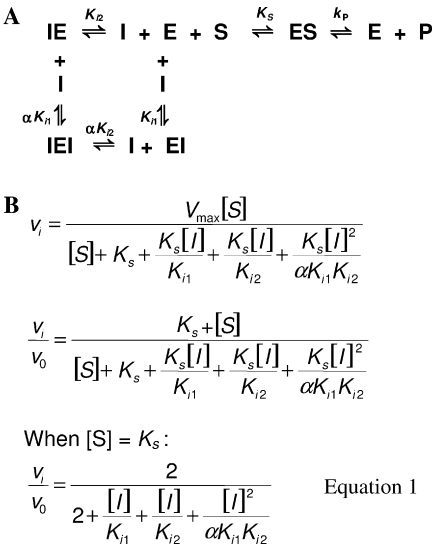

Figure 4. Cooperative pure competitive inhibition by two different non-exclusive inhibitors: (A) scheme of this mechanism under rapid equilibrium conditions; velocity equation for this system and the corresponding relation for $v_1/v_0 = f$ ([inhibitor]).

$v_i/v_0 = f$ ([inhibitor]) are shown in Figure 4B. This equation 1 fits very well our experimental data (the steeper curve in Figure 2B), which supports the above-mentioned two-site model.

This curve fitting yields a value of 0.42 mM[2] for the product $\alpha K_{i1}K_{i2}$, where K_{i1} and K_{i2} are the competitive inhibition constants for the interaction of Gln-KPA with GlnRS through its aminoacyl and AMP modules, respectively, and where α expresses the cooperativity between the binding of Gln-KPA at these two sites. If we assume that $\alpha = 1$ (i.e., no cooperativity), and that $K_{i1} = K_{i2}$, then we obtain an average value of 0.65 mM for the K_i of Gln-KPA with GlnRS (Fig. 2B). To obtain information on each of these three parameters, we sought to evaluate the inhibitory action of two inhibitors which share with Gln-KPA either its aminoacyl module or its AMP module. Glu-KPA fulfills the conditions for binding to the AMP-binding site of GlnRS and not to its amino acid-binding site; therefore, its K_i for *E. coli* GluRS (2.8 mM; see Fig. 2A and Table 1) is an estimate of K_{i2}. On the other hand, none of the glutamine analogs that we tested inhibited GlnRS. Therefore, we cannot estimate the value of α.

The unusual inhibitory properties of Gln-KPA for *E. coli* GlnRS (2 sites, and K_i of 0.65 mM) compared to those of Gln-ol-AMP[18] (1 site, $K_i = 280$ nM, structure on Scheme 2) and of Gln-AMS[19] (1 site and $K_i = 1.32$ μM, structure on Scheme 2) may be due to a steric hindrance between the hinge, connecting the two modules of this inhibitor, and the active site area of GlnRS, thus preventing the simultaneous binding of the two modules to each of their sites on this enzyme. This unusual Gln-KPA/GlnRS interaction, and the fact that the two modules of Glu-KPA can bind simultaneously to *E. coli* GluRS, reveals structural differences between the active sites of GlnRS and of GluRS. Considering that bacterial GlnRSs are evolutionarily closer to eukaryotic GluRSs than to bacterial GluRSs,[20–22] Glu-KPA could inhibit bacterial GluRSs much more efficiently than mammalian GluRSs. This model is supported by the fact that Glu-KPA does not inhibit significantly bovine liver GluRS (see below).

2.4. Inhibition of a mammalian cytoplasmic GluRS by Glu-KPA 9

Glu-KPA inhibits the cytoplasmic GluRS of calf liver, competitively with respect to glutamate (Fig. 2A, ◊), with a K_i of 2.6 mM. This inhibition is 145-fold weaker than that of *E. coli* GluRS (Table 1).

3. Discussion

Among all the known stable analogs of aminoacyl adenylates (aa-AMP) which inhibit aaRSs,[4] Gln-KPA is the only one for which the presence of two binding sites on the cognate aaRS (GlnRS) was revealed by inhibition kinetics. Considering the bimodular structure (aminoacyl and adenosine) of these inhibitors, this property of Gln-KPA suggests that its two structural modules cannot bind simultaneously to GlnRS. A possible model is that one Gln-KPA molecule binds GlnRS via its aminoacyl module, whereas the other binds it via its adenosine module (see Fig. 3). This model is consistent with the fact that GlnRS inhibition by Gln-KPA is 40-fold weaker than that of GluRS by Glu-KPA (Table 1) whose two modules can bind simultaneously to GluRS (Fig. 1). The joint binding of two covalently linked modules of a ligand to a protein is generally much stronger than that of each of the corresponding free modules; for instance, the covalent linking of the modules phenylalanine and AMP to form phenylalanyl adenylate leads to a much stronger binding of the latter ($K_d = 4$ nM) to phenylalanyl-tRNA synthetase than that of phenylalanine ($K_d = 30$ μM) or of AMP ($K_d = 1$ mM).[23]

The two main types of stable aa-AMP analogs that have been characterized as aaRS inhibitors are the aminoalkyl adenylates (aa-ol-AMP) and the aminoacylsulfamoyladenosines (aa-AMS).[4] In some cases, large differences between the K_i of the aa-ol-AMP and of the aa-AMS specific to a given aaRS have been reported; for instance, these values for *E. coli* GluRS are 3 μM and 2.8 nM, respectively.[24,25] The novel Glu-AMP analog presented here, Glu-KPA, has a K_i of 18 μM. These differences be-

tween aa-AMP analogs which share the same aminoacyl and adenosine modules but differ by the hinges linking them may be due to the binding properties of their hinges to the active site area, and/or their flexibility, including their vibrational modes on the enzyme.[26]

The only other aminoacyl-KPA characterized so far as an inhibitor is Asp-KPA.[9] It inhibits *E. coli* aspartyl-tRNA synthetase (AspRS) competitively with respect to aspartate. It has one binding site on this enzyme, and is much more efficient (K_i = 123 nM) than are Glu-KPA with GluRS (18 μM) and Gln-KPA with GlnRS (0.65 mM). As AspRS is a member of the class II aaRSs, which have no evolutionary linkage with the class I aaRSs[22] to whom GluRS and GlnRS belong, these inhibitory properties of Asp-KPA suggest that the linker between its two modules does not interfere with their optimal binding in the AspRS active site. It remains to be determined if this is a general property of the β-ketophosphonates (not yet synthesized) corresponding to the nine other class II aaRSs.

The facts that Glu-KPA and Glu-AMS inhibit *E. coli* GluRS much more efficiently than mammalian cytoplasmic GluRSs (Table 1) reveal the existence of important structural differences between the active sites of these orthologous enzymes. These differences make bacterial GluRSs promising targets for antimicrobial therapy.

4. Experimental

4.1. General

Chemical reagents were purchased from Aldrich–Sigma Chemical Company. Flash chromatography was carried out using 40–63 μM (230–400 mesh) silica gel. Optical rotations were measured using a JASCO DIP-360 digital polarimeter (c as g of compound per 100 mL). Infrared spectra were recorded on a Bomem MB-100 spectrometer. NMR spectra were recorded on a Varian Inova AS400 spectrometer (400 MHz).

For enzyme purification and assay, the following compounds were of the highest quality available and were purchased from the indicated companies: [14C]labeled L-amino acids from PerkinElmer Life and Analytical Sciences; unfractionated tRNA from *E. coli* MRE 600 and DNase I from Roche Diagnostics (Laval, Québec); unlabeled L-amino acids, ATP, the reducing agents 2-mercaptoethanol (2-ME) and dithiothreitol (DTT), and chicken egg white lysozyme from Sigma–Aldrich Canada Ltd; isopropyl 1-thio-β-D-galactopyranoside (IPTG), imidazole, and the buffers tris(hydroxymethyl)aminomethane (Tris) and 4-(2-hydroxyethyl)piperazine-1-ethanesulfonic acid (HEPES) from Laboratoire MAT (Beauport, Québec). Ni–NTA agarose columns from Qiagen Inc. (Canada).

4.2. Dimethyl β-ketophosphonate 6

To a solution of dimethyl methylphosphonate (0.43 mL, 3.97 mmol) in anhydrous THF (20 mL) at −78 °C was added dropwise (30 min) *n*-BuLi in hexane (2.5 M, 1.51 mL, 3.78 mmol). A solution of ester **5** (600 mg, 1.89 mmol) in THF (5 mL) was added and the solution was stirred at −78 °C for 1 h. The reaction was quenched by dropwise addition of satd aq NH_4Cl (30 mL) and THF was evaporated. The aqueous layer was extracted with ethyl acetate (3× 50 mL) and the organic layer was washed with satd aq NH_4Cl and brine, dried over $MgSO_4$, and evaporated. The crude product was purified by flash chromatography (gradient CH_2Cl_2/EtOAc, 3:2 to 1:1) to give **6** (555 mg, 72%) as a colorless oil: $[\alpha]_D^{21}$ 1.1 (*c* 3.3, $CHCl_3$); IR (neat) 3600–3100, 2978, 2929, 1713, 1518, 1250, 1158, 1031 cm^{-1}; ^1H NMR (400 MHz, $CDCl_3$) δ 1.26 (s, 18 H), 1.59–1.69 (m, 1H), 1.79–2.14 (m, 3H), 3.03 (dd, J = 22.0 and 14.4 Hz, 1H), 3.17 (dd, J = 22.6 and 14.4 Hz, 1H), 3.60 (d, J = 11.4 Hz, 3H), 3.61 (d, J = 11.4 Hz, 3H), 4.14–4.19 (m, 1H), 5.53 (d, J = 8.0 Hz, 1H); ^{13}C NMR (100 MHz, $CDCl_3$) δ 25.7, 28.0, 28.2, 31.2, 37.4 (d, J = 130.4 Hz), 52.9 (d, J = 6.9 Hz), 53.0 (d, J = 6.1 Hz), 59.6, 79.5, 80.3, 155.6, 172.0, 201.1 (d, J = 6.1 Hz); ^{31}P NMR (162 MHz, $CDCl_3$) δ 23.1; HRMS (CI, NH_3) calcd for $C_{17}H_{33}NO_8P$ $(M+H)^+$ 410.1944, found 410.1933.

4.3. Methyl β-ketophosphonate 7

A solution of dimethyl β-ketophosphonate **6** (558 mg, 1.36 mmol) in *tert*-butylamine (30 mL) was heated at reflux for 24 h. The solvent was evaporated and the solid residue was dissolved in CH_2Cl_2 (50 mL). A solution of HCl in dioxane (4 M, 0.34 mL, 1.36 mmol) was added and the mixture was diluted in ethyl acetate (100 mL). The organic phase was washed with brine, dried over $MgSO_4$, and evaporated. Flash chromatography (gradient EtOAc to MeOH/EtOAc, 2:3) provided **7** (507 mg, 94%) as a white solid: mp 103–105 °C; $[\alpha]_D^{21}$ 0.2 (*c* 0.55, MeOH), IR (KBr) 3600–3100, 2978, 2934, 1703, 1508, 1241, 1163, 1046 cm^{-1}; ^1H NMR (400 MHz, CD_3OD) δ 1.44–1.46 (m, 18H), 1.74–1.79 (m, 1H), 2.13–2.22 (m, 1H), 2.29–2.33 (m, 2H), 3.00 (dd, J = 21.2 and 12.8 Hz, 1H), 3.18 (dd, J = 21.8 and 12.8 Hz, 1H), 3.59 (d, J = 10.9 Hz, 3H), 4.39–4.44 (m, 1H); ^{13}C NMR (100 MHz, CD_3OD) δ 26.9, 28.5, 28.9, 32.7, 52.5 (d, J = 5.6 Hz), 60.6, 80.9, 81.7, 158.1, 174.2, 206.8 (d, J = 5.4 Hz); ^{31}P NMR (162 MHz, CD_3OD) δ 16.6; LRMS (ESI) 418.1 $(M+Na)^+$.

4.4. Phosphonate 8

To a solution of **7** (350 mg, 0.855 mmol) in anhydrous DMF (2 mL) were added 2′,3′-isopropylideneadenosine (408 mg, 1.32 mmol), HBTU (402 mg, 1.06 mmol), and *i*-Pr_2NEt (0.62 mL, 3.54 mmol), and the solution was stirred at room temperature for 8.5 h. The reaction mixture was diluted with AcOEt (120 mL), washed with 1 M HCl, satd aq $NaHCO_3$, brine, and the organic layer was dried ($MgSO_4$), and evaporated. The crude product was purified by flash chromatography (EtOAc to 20% MeOH/AcOEt) to give the coupled product partially contaminated by 2′,3′-isopropylideneadenosine. This mixture was stirred with pyridine/H_2O (27 mL/3 mL) at 55°C for 10 h. The solvents were evaporated and

the residue was purified by flash chromatography (15% MeOH/CH_2Cl_2 to 40% MeOH/CH_2Cl_2) to give **8** (208 mg, 35%) as a white solid: mp 147 °C (dec); $[\alpha]_D^{21}$ −34.7 (*c* 0.65, MeOH); IR (KBr) 3600–3100, 1709, 1212, 1156, 1064, 856 cm^{-1}; ^1H NMR (400 MHz, CD_3OD) δ 1.35–1.41 (m, 21H), 1.57 (s, 3H), 1.65–1.75 (m, 1H), 2.08–2.17 (m, 1H), 2.19–2.25 (m, 2H), 2.85–3.18 (m, 2H), 4.04–4.08 (m, 2H), 4.32–4.37 (m, 1H), 4.44 (br s, 1H), 4.85–5.11 (m, 1H), 5.28 (dd, J = 6.0 and 3.2 Hz, 1H), 6.17–6.19 (m, 1H), 8.18 (s, 1H), 8.44 (s, 1H); ^{13}C NMR (100 MHz, CD_3OD) δ 24.4, 25.5, 26.3, 27.2, 27.6, 31.3, 59.3, 59.4, 64.6, (d, J = 4.8 Hz), 64.7 (d, J = 4.8 Hz), 79.6, 79.7, 80.43, 80.45, 82.0, 82.1, 84.55, 84.56, 85.5 (d, J = 7.6 Hz), 90.6, 113.9, 114.0, 119.0, 140.3, 140.4, 149.2, 149.3, 152.8, 156.1, 156.7, 156.8, 172.9, 205.0; ^{31}P NMR (162 MHz, CD_3OD) δ 18.0; HRMS (FAB) calcd for $C_{28}H_{44}N_6O_{11}P$ $(M+H)^+$ 671.2805, found 671.2800.

4.5. Glutamic ketophosphonate 9

A solution of compound **8** (40 mg, 59.6 μmol) in trifluoroacetic acid/water (9 mL/1 mL) was stirred at room temperature for 15 min. The solvents were evaporated under reduced pressure. The residue was co-evaporated with water, then with MeOH/Et_2O to give **9** (34 mg, 97%) as a white solid: mp 122 °C (dec); $[\alpha]_D^{21}$ −21.4 (*c* 1.0, DMF); IR (KBr) 3600– 2800, 1684, 1201, 1130 cm^{-1}; ^1H NMR (400 MHz, D_2O) δ 1.87–1.96 (m, 1 H), 2.16–2.26 (m, 1H), 2.33–2.40 (m, 2H), 3.96–4.06 (m, 2H), 4.18–4.21 (m, 1H), 4.22–4.25 (m, 1H), 4.29–4.33 (m, 1H), 4.55–4.58 (m, 1H), 6.00 (d, J = 5.0 Hz, 1H), 8.25 (s, 1H), 8.42 (s, 1H); ^{13}C NMR (100 MHz, D_2O) δ 23.6, 29.08, 29.12, 38.2–40.0 (m, C–D coupling, H–D exchange with D_2O), 58.8, 64.0, 64.1, 64.2, 69.9, 70.0, 74.51, 74.54, 83.7 (d, J = 7.6 Hz), 88.3, 88.4, 116.2 (q, J = 289.0 Hz, TFA), 118.53, 118.54, 142.48, 142.53, 144.7, 148.23, 148.24, 149.8, 162.6 (q, J = 35.0 Hz, TFA), 175.8, 175.9, 200.9, 201.0; ^{31}P NMR (162 MHz, D_2O) δ 16.1; LRMS (ESI) 475.1 $(M+H)^+$.

4.6. Glutamine methyl ester 11

N-α-Boc-*N*-γ-trityl-L-glutamine **10** (2.62 g, 5.36 mmol) was dissolved in MeOH/H_2O (10:1, 35 mL) and the solution was titrated to pH 7.0 with a 20% aqueous solution of Cs_2CO_3. The solvents were evaporated and the residue co-evaporated with toluene. The solid cesium salt was stirred with methyl iodide (0.370 mL, 5.90 mmol) in dry DMF (25 mL) for 1 h at room temperature. The reaction mixture was diluted with EtOAc (250 mL) and the organic phase was washed with satd aq $NaHCO_3$ and brine, dried over $MgSO_4$, evaporated, and then co-evaporated with toluene to remove residual DMF. The crude product was purified by flash chromatography (CH_2Cl_2/EtOAc, 10:1) to give **11** (2.37 g, 88%) as a white solid: mp 153–154 °C, lit.[15] 153–154 °C; $[\alpha]_D^{21}$ 15.2 (*c* 1.01, $CHCl_3$); IR (KBr) 3600–3100, 2971, 1746, 1714, 1638, 1210, 710 cm^{-1}; ^1H NMR (400 MHz, $CDCl_3$) δ 1.44 (s, 9H), 1.80–1.96 (m, 1H), 2.11–2.26 (m, 1H), 2.28–2.49 (m, 2H), 3.72 (s, 3H), 4.27–4.38 (m, 1H), 5.24 (d, J = 7.6 Hz, 1H), 7.13 (s, 1H), 7.17–7.39 (m, 15H); ^{13}C NMR (100 MHz, $CDCl_3$) δ 28.3, 29.2, 33.7, 52.5, 70.7, 80.2, 127.0, 128.2, 129.0, 144.7, 155.9, 170.9, 172.8.

4.7. Dimethyl β-ketophosphonate 12

To a solution of dimethyl methylphosphonate (10.40 mL, 96.00 mmol) in anhydrous THF (70 mL) at −78 °C was added dropwise *n*-BuLi in hexane (1.6 M, 60.00 mL, 96.00 mmol) and the mixture was stirred for 45 min. A solution of ester **11** (2.01 g, 4.00 mmol) in anhydrous THF (100 mL) was added and the solution was stirred at −78 °C for 1 h, then at −30 °C for another 1 h. The reaction was quenched by the addition of saturated aqueous NH_4Cl (50 mL). The reaction mixture was extracted with ethyl acetate and the organic phase was washed with water, brine, dried over $MgSO_4$, and concentrated to 20 mL. Petroleum ether was added and filtration after 24 h at room temperature provided **12** (1.92 g, 81%) as a white solid: mp 181–182°C, lit.[15] 183–184°C; $[\alpha]_D^{21}$ −18.9 (*c* 1.08, MeOH); IR (KBr) 3600–3100, 3030, 2978, 2957, 1717, 1674, 1650, 1256, 1035 cm^{-1}; ^1H NMR (400 MHz, $CDCl_3$) δ 1.43 (s, 9H), 1.73–1.90 (m, 1H), 2.13–2.29 (m, 1H), 2.30–2.51 (m, 2H), 3.06 (dd, J = 21.8 and 14.4 Hz, 1H), 3.24 (dd, J = 22.2 and 14.5 Hz, 1H), 3.73 (d, J = 11.1 Hz, 3H), 3.75 (d, J = 11.3 Hz, 3H), 4.27–4.37 (m, 1H), 5.55 (d, J = 7.1 Hz, 1H), 7.16–7.35 (m, 15H); ^{13}C NMR (100 MHz, $CDCl_3$) δ 27.0, 28.3, 33.1, 37.7 (d, J = 134.1 Hz), 53.1, 60.1, 70.6, 80.3, 127.0, 127.9, 128.8, 144.7, 155.9, 171.2, 201.1 (d, J = 6.2 Hz); ^{31}P NMR (162 MHz, $CDCl_3$) δ 23.0.

4.8. Methyl β-ketophosphonate 13

To a solution of phosphonate **12** (1.60 g, 2.70 mmol) in THF/DMF (15 mL/5 mL) were added triethylamine (2.00 mL) and benzenethiol (1.00 mL). The solution was stirred at room temperature for 48 h. The solvents were evaporated and then co-evaporated with toluene. The crude product was purified by flash chromatography (1% Et_3N/10% MeOH/ 89% CH_2Cl_2) to give **13** (1.82 g, 98%) as a white solid: mp 156–158 °C; $[\alpha]_D^{21}$ −0.5 (*c* 1.04, MeOH); IR (KBr) 3600–3100, 3058, 2981, 2948, 2678, 2491, 1697, 1492, 1214, 1167, 1050, 701 cm^{-1}; ^1H NMR (400 MHz, $CDCl_3$) δ 1.27 (t, J = 7.3 Hz, 9H), 1.42 (s, 9H), 1.78–1.94 (m, 1H), 2.21–2.40 (m, 3H), 2.86 (dd, J = 20.9 and 12.1 Hz, 1H), 2.94–3.06 (m, 6H), 3.34 (dd, J = 21.9 and 12.2 Hz, 1H), 3.59 (d, J = 11.1 Hz, 3H), 4.30–4.40 (m, 1H), 6.77 (d, J = 8.0 Hz, 1H), 7.17–7.33 (m, 15H), 7.39 (s, 1H), 12.01 (br s, 1H); ^{13}C NMR (100 MHz, $CDCl_3$) δ 8.5, 28.3, 28.4, 33.8, 41.0 (d, J = 112.4 Hz), 45.6, 52.3, 59.9, 70.4, 80.0, 126.8, 127.8, 128.8, 144.9, 156.3, 171.6, 204.8; ^{31}P NMR (162 MHz, $CDCl_3$) δ 13.6; LRMS (ESI) 682.3 $(M+H)^+$.

4.9. Phosphonate 14

A solution of phosphonate **13** (0.830 g, 1.17 mmol), isopropylideneadenosine **1** (0.504 g, 1.64 mmol), DMAP (0.162 g, 1.33 mmol), and HBTU (1.33 g, 3.51 mmol) in anhydrous DMF (8 mL) was stirred at room temperature for 3.5 h. The mixture was partitioned between

ethyl acetate and saturated aqueous NH_4Cl and the organic layer was washed with brine, dried over $MgSO_4$, evaporated, and then co-evaporated with toluene. The product was purified by flash chromatography (2%MeOH in CH_2Cl_2 to 5%MeOH in CH_2Cl_2). To a solution of this product in DMF (6 mL) were added triethylamine (0.50 mL) and benzenethiol (0.25 mL), and the mixture was stirred at room temperature for 24 h. The solution was evaporated and then co-evaporated with toluene. The crude product was purified by flash chromatography (1%Et_3N/20%MeOH/79%CH_2Cl_2) to give phosphonate **14** (0.923 g, 57% for 2 steps) as a white solid: mp 169–171 °C; $[\alpha]_D^{21}$ −25.0 (*c* 1.04, MeOH); IR (KBr) 3600–3100, 3058, 2978, 2936, 2678, 1691, 1491, 1214, 1164, 1064 cm^{-1}; ^1H NMR (400 MHz, $CDCl_3$) δ 1.20 (t, $J = 7.3$ Hz, 9 H), 1.35 (s, 3H), 1.40 (s, 9H), 1.61 (s, 3H), 1.77–1.95 (m, 1H), 2.22–2.41 (m, 3H), 2.74–2.92 (m, 1H), 2.95 (q, $J = 7.3$ Hz, 6H), 3.20–3.38 (m, 1H), 3.98–4.12 (m, 2H), 4.29–4.43 (m, 1H), 4.45–4.53 (m, 1H), 5.03–5.11 (m, 1H), 5.13–5.23 (m, 1H), 6.20–6.26 (m, 1H), 6.48 (br s, 2H), 7.10–7.32 (m, 15H), 7.44 (d, $J = 9.2$ Hz, 1H), 8.29 (s, 1H), 8.37 (s, 1H); ^{13}C NMR (100 MHz, $CDCl_3$) δ 8.5, 25.3, 27.2, 28.4, 29.7, 33.7, 41.5 (d, $J = 113.6$ Hz), 45.6, 59.9, 65.0, 70.4, 79.6, 81.7, 85.0, 85.8, 90.8, 114.0, 119.4, 126.8, 127.8, 128.8, 139.9, 144.8, 149.5, 152.3, 155.1, 156.3, 171.6, 204.9; ^{31}P NMR (162 MHz, $CDCl_3$) δ 12.0; LRMS (ESI) 856.3 $(M+H)^+$.

4.10. β-Ketophosphonate 15

A solution of compound **14** (142 mg, 0.242 mmol) in trifluoroacetic acid/water (5.4 mL/0.6 mL) was stirred at room temperature for 15 min. The solvents were evaporated under reduced pressure and the solid residue co-evaporated with Et_2O/MeOH. The crude product was dissolved in a minimum of MeOH and precipitated by the addition of Et_2O (10 mL). The precipitate is filtered and washed with Et_2O/MeOH to give **15** as a white solid (78 mg, 68%): mp 133–135 °C (dec); $[\alpha]_D^{21}$ −8.2 (*c* 0.10, H_2O); IR (KBr) 3600–2700, 2977, 2934, 1677, 1203, 1132, 1065 cm^{-1}; ^1H NMR (400 MHz, D_2O) δ 2.04–2.17 (m, 1H), 2.27–2.53 (m, 3H), 3.03–3.45 (m, 2H), 4.16–4.24 (m, 2H), 4.36–4.44 (m, 2H), 4.49–4.55 (m, 1H), 4.72–4.84 (m, 1H), 6.17 (d, $J = 5.1$ Hz, 1H), 8.37 (s, 1H), 8.55–8.56 (2s, 1H); ^{13}C NMR (100 MHz, D_2O) δ 27.1, 33.1, 42.7 (d, $J = 116.8$ Hz), 61.7, 66.9, 72.9, 77.2, 86.8, 91.1, 121.5, 145.4, 147.6, 151.2, 152.8, 176.1, 204.0; ^{31}P NMR (162 MHz, D_2O) δ 15.9; LRMS (ESI) 474.1 $(M+H)^+$.

4.11. Enzyme purifications

Glutamyl-tRNA synthetase (GluRS): The *E. coli* His-tagged GluRS was produced in the *E. coli* strain JP1449[DE3]pLysS containing the pET28cTXERS plasmid (Dubois, D.Y., unpublished results), by induction with 0.5 mM IPTG at $A_{600\ nm} = 0.4$ and overnight culture at room temperature to avoid the formation of inclusion bodies. Cells were resuspended in 20 mM Tris–HCl buffer (pH 7.9) containing 5 mM imidazole. The lysis was performed by the addition of lysozyme from chicken egg white and one tablet of 'Complete, Mini, EDTA-free protease inhibitor cocktail' (Roche Diagnostics). DNase I was added to the lysate and the mixture stirred on ice until the viscosity was significantly reduced; then, 1 mM 2-ME was added. The lysate was centrifuged for 45 min at 17500*g*, and the supernatant was clarified by passage through a 0.22 μm filter. The enzyme was purified by affinity chromatography on a 5 ml Ni–NTA agarose column equilibrated in 20 mM Tris–HCl (pH 7.9) and 5 mM imidazole. The column was successively washed with this Tris buffer containing 5 and 25 mM imidazole. The enzyme was eluted with 1 M imidazole in the same buffer. The washing and elution buffers also contain 1 mM 2-ME. The GluRS was concentrated and dialyzed against the storage buffer (20 mM HEPES–KOH, pH 7.2, 45% glycerol, and 5 mM 2-ME).

Glutaminyl-tRNA synthetase (GlnRS): The gene of the *E. coli* His-tagged GlnRS cloned in the pQRST plasmid (kindly provided by Prof. John Perona, Univ. Calif. Santa Barbara) was over-expressed in BL21[DE3]pLysS by induction with 1 mM IPTG at $A_{600\ nm} = 0.5$ for 4 h at 37°C. Cells were resuspended in 50 mM HEPES–KOH buffer (pH 7.2) containing 0.5 M NaCl, 10 mM imidazole, and 15 mM $MgCl_2$. The lysis and protein extract preparation were performed as for the GluRS. The purification and storage of the enzyme were performed as described.[27]

Mammalian GluRS and tRNA: A partially purified fraction of bovine liver containing aaRSs was obtained from Bio S&T Inc. (Montreal, Canada). Transfer RNA from calf liver was obtained from Sigma–Aldrich Canada Ltd.

4.12. Enzyme activity and inhibition assays

E. coli. GluRS: The tRNA glutamylation reactions were carried out in 50 mM HEPES–KOH, pH 7.2, 16 mM $MgCl_2$, 2 mM ATP, 3 mM DTT, 5 μM $tRNA^{Glu}$ in *E. coli* tRNA, and 50–400 μM L-[^{14}C(U)]glutamate (adapted from Tremblay and Lapointe[28]). The reaction was initiated by adding the pre-incubated enzyme to a final concentration of 2 nM. The amount of glutamyl-tRNA formed was determined by measuring the radioactivity present in 5% trichloroacetic acid precipitates of reaction mixture aliquots, as previously described.[29] The initial rates of the reaction were determined by measuring the amounts of [^{14}C]glutamyl-tRNA formed in 40 μl aliquots taken at 2 min intervals over 12 min. The inhibitor, Glu-KPA **9**, freshly prepared as a 25 mM solution in 50 mM HEPES–KOH, pH 7.2 buffer, was added at various final concentrations (0–200 μM) just before pre-incubating the reaction medium at 37 °C for 2 min. No significant decrease of inhibitory activity was observed for Glu-KPA after 10 months in the above buffer at 4 °C. Analysis of this fraction by electrophoresis on polyacrylamide gel in the presence of sodium dodecyl sulfate (SDS–PAGE) (Fig. 5) indicates that this GluRS is pure, as it migrates as a single band, and has the expected molecular mass of about 55 kDa with the $(His)_6$ tag.[30]

Mammalian GluRS: The aminoacylation reactions were carried out in 50 mM HEPES–KOH, pH 7.2, 50 mM

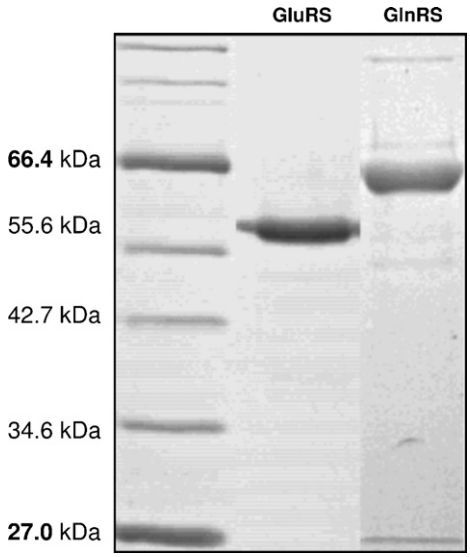

Figure 5. SDS–PAGE (10%) of the purified fractions of *E. coli* GluRS and GlnRS (5 μg per lane).

KCl, 10 mM ATP, 8 mM $MgCl_2$, 3 mM DTT, 0.1 mg/ml BSA, and 192 μM L-[^{14}C(U)]glutamate (the K_m value). The partially purified fraction of bovine liver aaRSs was added in a proportion of 2% v/v. The reaction was initiated after a 20 min pre-incubation period at 37 °C, by the addition of 100 μM of pre-incubated, unfractionated calf liver tRNA. Aliquots of 20 μl were taken at 5 min intervals and treated as described for the *E. coli* GluRS assay.

E. coli. GlnRS: The tRNA glutaminylation reactions were carried out as described above for GluRS, except for the following differences in the reaction medium: 50 mM HEPES–KOH, pH 7.2, 10 mM Mg acetate, 2 mM ATP, 6 μM $tRNA^{Gln}$ in *E. coli* MRE 600 unfractionated tRNA, and 15–100 μM L-[3,4-^{3}H(N)]glutamine (adapted from Hong et al.[31]). The enzyme was added to a final concentration of 1 nM. The inhibitor, Gln-KPA **15**, freshly prepared as a 25 mM solution in 50 mM HEPES–KOH, pH 7.2, buffer, was added at various final concentrations (0–1.5 mM). Analysis of this fraction by SDS–PAGE (Fig. 5) indicates that this GlnRS is pure, as it migrates as a single band, and has the expected molecular mass of about 64.2 kDa with the $(His)_6$ tag.[32]

4.13. Determination of the inhibition type and constant (K_i)

The K_m and K_m^{app} for the amino acid substrate were first calculated from Lineweaver–Burk plots. The K_m values for the amino acids were, respectively, of 113 μM for the GluRS and 25 μM for the GlnRS. The K_i values were calculated from the K_m^{app} vs [I] plot. The K_i values for the inhibitors with respect for the amino acid substrates were determined by measuring the apparent K_m for the amino acid in the presence of saturating concentrations of both ATP and tRNA, and of various fixed concentrations of the inhibitor. Alternatively, the rate 'v_i' of the aminoacylation reaction in the presence of various inhibitor concentrations [I] was determined at the amino acid concentration corresponding to K_m, in the presence of saturating concentrations of both ATP and tRNA, and the ratio v_i/v_0 (where v_0 is the rate in the absence of inhibitor under the same substrate concentrations) was plotted as a function of [I]. Curve-fitting of these data using the theoretical functions for v_i/v_0 for various types of inhibition[16] was made with the software Kaleidagraph (version 4.0) and was used to identify the types of inhibition and the K_i values.

For competitive inhibition with one binding site for the inhibitor, the velocity equation for this system under rapid equilibrium conditions, and the corresponding relation for $v_i/v_0 = f$ ([inhibitor]) are:

$$v_i = \frac{V_{max}[S]}{[S] + K_m(1 + \frac{[I]}{K_i})}$$

$$\frac{v_i}{v_0} = \frac{[S] + K_m}{[S] + K_m(1 + \frac{[I]}{K_i})}$$

$$\text{When } [S] = K_m \frac{v_i}{v_0} = \frac{2}{2 + \frac{[I]}{K_i}} \quad \text{Equation 2}$$

This last equation was used for the curve-fittings presented in Figure 2, except for the left curve of Figure 2B and for the curve in Figure 2A describing mammalian GluRS inhibition (◊).

Acknowledgments

This work was supported by Grant OGP 0009597 from the Natural Sciences and Engineering Research Council of Canada (NSERC, to J. L.) and by Grant PR-105-092 from the "Fonds de recherche sur la nature et les technologies, Québec" (to R. C. and J. L.).

References and notes

1. Ibba, M.; Söll, D. *Annu. Rev. Biochem.* **2000**, *69*, 617.
2. Martinis, S. A.; Plateau, P.; Cavarelli, J.; Florentz, C. *Biochimie* **1999**, *81*, 683.
3. Eriani, G.; Delarue, M.; Poch, O.; Gangloff, J.; Moras, D. *Nature* **1990**, *347*, 203.
4. Chênevert, R.; Bernier, S.; Lapointe, J. In *Translation Mechanisms*; Lapointe, J., Brakier Gingras, L., Eds.; Landes Bioscience/Kluwer Academic: Georgetown, TX/New York, 2003; pp 416–428.
5. Kim, S.; Lee, S. W.; Choi, E. C.; Choi, S. Y. *Appl. Microbiol. Biotechnol.* **2003**, *61*, 278.
6. Hurdle, J. G.; O'Neill, A. J.; Chopra, I. *Antimicrob. Agents Chemother.* **2005**, *49*, 4821.
7. Hugues, J.; Mellow, G. *Biochem. J.* **1980**, *191*, 209.
8. Jarvest, R. L.; Berge, J. M.; Berry, V.; Boyd, H. F.; Brown, M. J.; Elder, J. S.; Forrest, A. K.; Fosberry, A. P.; Gentry, D. R.; Hibbs, M. J.; Jaworsky, D. D.; O'Hanlon, P. J.; Pope, A. J.; Rittenhouse, S.; Sheppard, R. J.; Slater-Radosti, C.; Worby, A. *J. Med. Chem.* **2002**, *45*, 1959.
9. Bernier, S.; Akochy, P. M.; Lapointe, J.; Chênevert, R. *Bioorg. Med. Chem.* **2005**, *13*, 69.
10. Southgate, C. C. B.; Dixon, H. B. F. *Biochem. J.* **1978**, *175*, 461.

11. Chauvel, E. N.; Coric, P.; Llorens-Cortes, C.; Wilk, S.; Roques, B. P.; Fournie-Zalusky, M. C. *J. Med. Chem.* **1994**, *37*, 1339.
12. Gray, M. D. M.; Smith, D. J. H. *Tetrahedron Lett.* **1980**, *21*, 859.
13. Vercerkova, H.; Smrt, J. *Collect. Czech. Chem. Commun.* **1983**, *48*, 1323.
14. Wang, S. S.; Gisin, B. F.; Winter, D. P.; Makofske, R.; Kulesha, I. D.; Tzougraki, C.; Meienhofer, J. *J. Org. Chem.* **1997**, *42*, 1286.
15. Brewer, H.; James, C. A.; Rich, D. H. *Org. Lett.* **2004**, *6*, 4779.
16. Segel, I. H. *Enzyme kinetics*; John Wiley: New York, 1975.
17. Dubois, D. Y.; Lapointe, J.; Sekine, S. I. In *The Aminoacyl-tRNA Synthetases*; Ibba, M., Francklyn, C., Cusack, S., Eds.; Landes Bioscience: Georgetown, Texas, 2005, chapter 10.
18. Bernier, S.; Dubois, D.; Therrien, M.; Lapointe, J.; Chênevert, R. *Bioorg. Med. Chem. Lett.* **2000**, *10*, 2441.
19. Rath, V. L.; Silvian, L. F.; Beijer, B.; Sproat, B. S.; Steitz, T. A. *Structure* **1998**, *6*, 439.
20. Lamour, V.; Quevillon, S.; Diriong, S.; N'Guyen, V. C.; Lipinski, M.; Mirande, M. *Proc. Natl. Acad. Sci. U.S.A.* **1994**, *91*, 8670.
21. Gagnon, Y.; Lacoste, L.; Champagne, N.; Lapointe, J. *J. Biol. Chem.* **1996**, *271*, 14856.
22. Woese, C. R.; Olsen, G. J.; Ibba, M.; Söll, D. *Microbiol. Mol. Biol. Rev.* **2000**, *64*, 202.
23. Lin, S. X.; Baltzinger, M.; Remy, P. *Biochemistry* **1983**, *22*, 681.
24. Desjardins, M.; Garneau, S.; Desgagnés, J.; Lacoste, L.; Yang, F.; Lapointe, J.; Chênevert, R. *Bioorg. Chem.* **1998**, *26*, 1.
25. Bernier, S.; Dubois, D. Y.; Habegger-Polomat, C.; Gagnon, L. P.; Lapointe, J.; Chênevert, R. *J. Enzym. Inhib. Med. Chem.* **2005**, *20*, 61.
26. Schramm, V. L. *Curr. Opin. Struct. Biol.* **2005**, *15*, 604.
27. Uter, N. T.; Gruic-Sovulj, I.; Perona, J. J. *J. Biol. Chem.* **2005**, *280*, 23966.
28. Tremblay, T. L.; Lapointe, J. *Biochem. Cell. Biol.* **1986**, *64*, 315.
29. Lapointe, J.; Levasseur, S.; Kern, D. *Methods Enzymol.* **1985**, *113*, 42.
30. Breton, R.; Papayannopoulos, I.; Biemann, K.; Lapointe, J. *J. Biol. Chem.* **1986**, *261*, 10610.
31. Hong, K. W.; Ibba, M.; Weygand-~~D~~uraševic, I.; Rogers, M. J.; Thomann, H. U.; Söll, D. *EMBO J.* **1996**, *15*, 1983.
32. Rould, M. A.; Perona, J. J.; Söll, D.; Steitz, T. A. *Science* **1989**, *246*, 1135.